Organic & Biomolecular Chemistry

www.rsc.org/obc

Volume 6 | Number 15 | 7 August 2008 | Pages 2641–2828

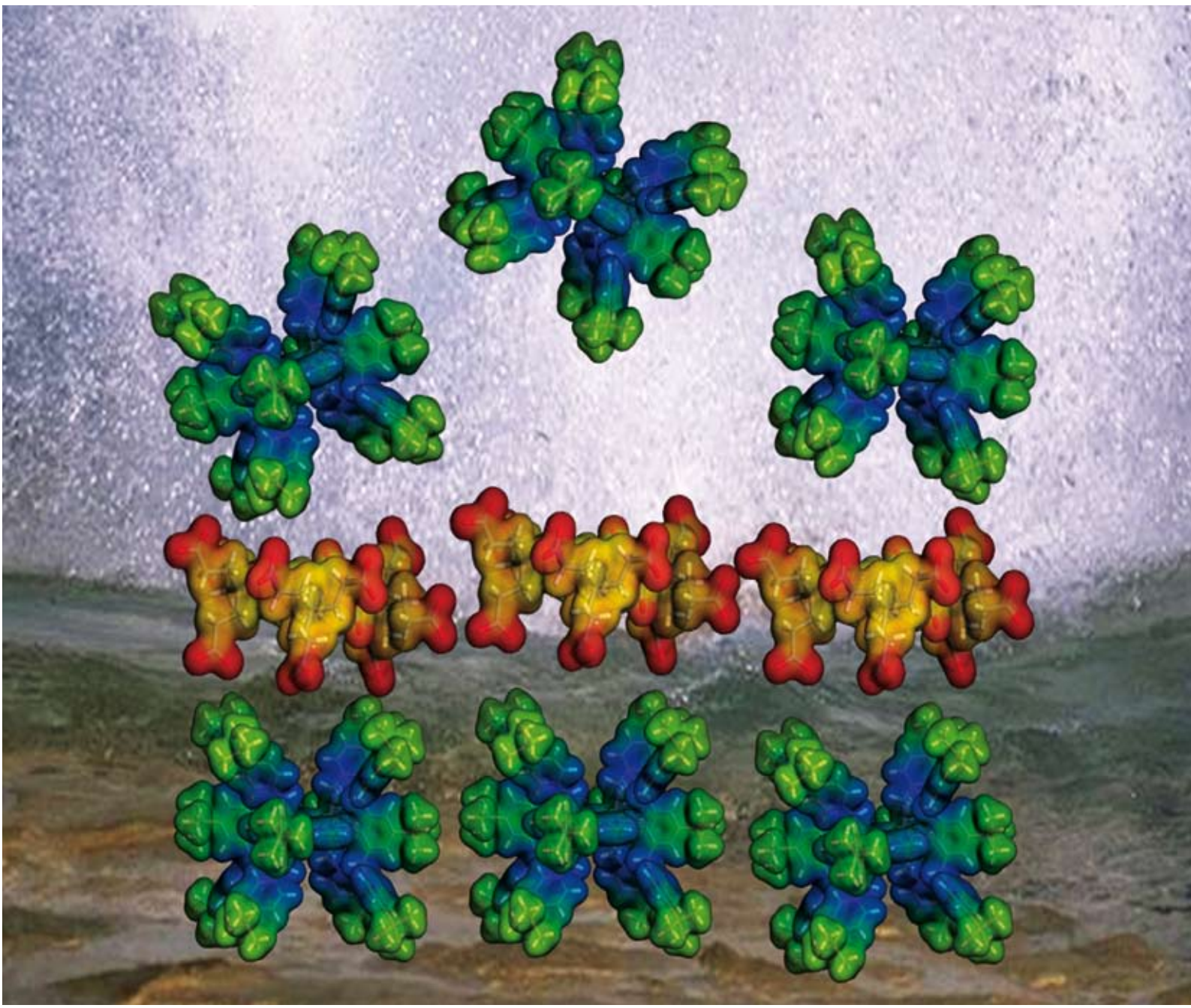

ISSN 1477-0520

FULL PAPER

Karin Rosenlehner *et al.*

Layer-by-layer deposition of molecular oligoelectrolytes—investigation of assembling and degradation behaviour

Chemical Biology

In this issue...

1477-0520(2008)6:15;1-I

RSC Publishing

Layer-by-layer deposition of molecular oligoelectrolytes—investigation of assembling and degradation behaviour

Karin Rosenlehner, Torsten Schunk, Norbert Jux, Michael Brettreich and Andreas Hirsch*

Received 12th March 2008, Accepted 28th April 2008
First published as an Advance Article on the web 29th May 2008
DOI: 10.1039/b804290j

The assembly and degradation behavior of oligoelectrolyte multilayer films (OEMs) self assembled by layer-by-layer deposition of positively and negatively charged oligoelectrolytes **1–6** was investigated. Next to colorless oligoelectrolytes we have employed representatives involving chromophores, in particular porphyrins. This allows for the systematic observation of both assembly and disassembly of the OEMs using optical spectroscopy, where chromophore containing building blocks serve as reporter electrolytes. The OEMs investigated in this study were built in a consistent, monomolecular matter and show linear correlation between the absorption and the number of layers. Using the concept of reporter electrolytes we have introduced for the first time also the use of non-chromophoric oligoelectrolytes, such as the new synthesized cationic system **2** as building blocks for OEMs. Moreover, we have investigated for the first time the degradation behavior of OEMs. We demonstrated that two different mechanisms of degradation proceed at the same time. The direct degradation is accompanied by a second release mechanism.

Introduction

The search for new methods for the deposition of thin films with precise control over the supramolecular assembly of the constituting molecular building block films has led to the simple but very efficient wet-coating layer-by-layer (LbL) technique.[1] Due to the interplay of electrostatic attraction and repulsion, oppositely charged polyions can be self-assembled on solid surfaces of, for example, glass or metals.[2] Iterative dipping circles lead to the deposition of thin films composed of alternating monolayers of polycations and polyanions. This promising new method convinces through its versatility and simplicity and offers a novel approach to advanced materials based on polyelectrolyte multilayer films (PEMs) in an easy and cheap way. Investigations on the use of LbL modified materials for biomedical applications including new concepts for drug delivery were recently reviewed by Tang *et al.*[3] Since polyelectrolyte films can also be loaded with dyes,[4,5] their performance as controlled release systems could be studied. The recent progress report by Lynn[6] concentrates on different types of erosion and disassembly of multilayered polyelectrolyte thin films from rapid and triggered to sustained and sequential release. Due to different types of erosion, control over the administration of different agents in one film is conceptually possible.[6] However, one inherent limitation of the current LbL-method is the use of polymers as charged building blocks. They are polydisperse and usually do not adopt a defined and controllable shape and orientation within the deposited layers. This leads to restrictions for precise fine tuning of the thin film properties and the manageability of polymeric thin films is therefore very demanding as was recently pointed out by, for example, Park *et al.*[7] In this investigation, inhomogeneous layers of polymers with dissimilar charge density were observed. We have recently extended the LbL-concept to monodisperse oligoelectrolytes with defined structures and number of charges.[8–14] Implicit to non-polymeric molecular oligoelectrolytes is the fact that the molecular structures can be varied and as a consequence, their behavior within the films can be widely modified. For example, features such as color or amphiphilic behavior can easily be introduced by employing additional molecular dye building blocks or hydrophobic moieties. The oligoelectrolytes that we used for the LbL-assembly are mainly based on Newkome or Newkome-type dendritic structures.[15,16] These perfect monodisperse molecules possess a regular and highly branched structure and thus can be used for various implementations in supramolecular aggregation chemistry. Fullerene-linked amphiphiles containing polar dendritic head groups were found to form stable single-layer (unilamellar) vesicles as a new class of artificial lipids.[8] Similar amphifullerenes form stable aggregates with positively charged proteins like cytochrome c as we found out through photophysical investigations like fluorescence spectroscopy and transient absorption spectroscopy.[9] The high electrostatic interaction and complexation between anionic and cationic oligoelectrolytes was investigated in a very detailed manner by gel electrophoresis measurements.[12] The strong electrostatic complexation between the anionic Newkome type dendritic building blocks and cationic oligoelectrolytes was also exploited for the construction of an electrostatically arranged ITO photoelectrode that reversibly transmits and processes solar energy.[13] A multicomponent redox gradient on an ITO glass surface could be formed through electrostatic assembly of redox active oligoelectrolytes. These devices exhibit remarkable efficiencies with respect to photon to current conversion.[14,17]

Department of Chemistry and Pharmacy & Interdisciplinary Center for Molecular Materials (ICMM) Friedrich-Alexander Universität Erlangen-Nürnberg, Henkestrasse 42, 91054, Erlangen, Germany. E-mail: andreas.hirsch@chemie.uni-erlangen.de; Fax: +49 9131 8526864

In this contribution, we wish to present a detailed study on the LbL-assembly and disassembly of a library of oligoelectrolytes (formulas **1**–**6**) in order to demonstrate the general feasibility of this concept for the construction of oligoelectrolyte multilayer films (OEMs). A key point of this study is the application of so-called reporter oligoelectrolytes, which allow for precise monitoring of the successive film assembly using optical spectroscopy. Next to their assembly, we present the first investigation of the disassembly of OEMs. These investigations are motivated by the idea of incorporating bioactive molecules at a certain inter-layer position of OEMs, which after the removal of the outer layers can be released to the environment. Such a drug delivery concept is of great interest for biomedical applications, for example, future transplantation technology.

Results and discussion

1. Synthesis of molecular oligoelectrolytes

The molecules used in this study (formulas **1**–**6**) contain as charged moieties either carboxylates or pyridinium groups. These can be arranged either within Newkome-like dendrimers (**1**–**4**) or evenly distributed substitutents around a tetraphenylporphyrin architecture (**5**, **6**). The negatively charged carboxylates are formed from the corresponding acids by dissolution in an aqueous buffer at neutral pH. We have already reported in previous contributions the synthesis of the oligoelectrolytes **1**, **3**–**6**.[10,11,14,17] Whereas the access to Newkome-like dendrimers with peripheric carboxylic groups is quite straightforward, no cationic representatives have

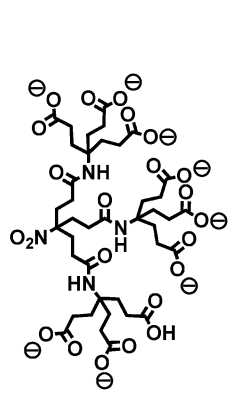

1

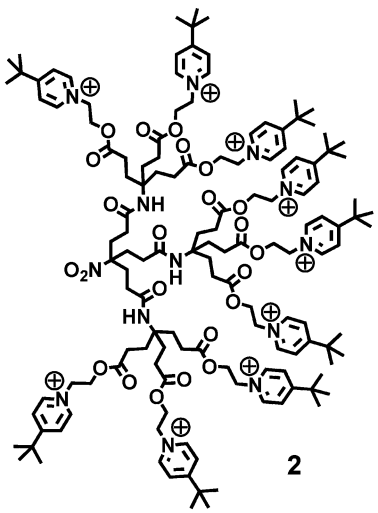

2

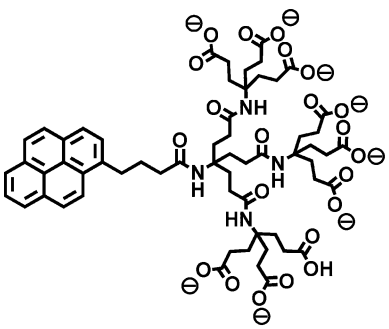

3

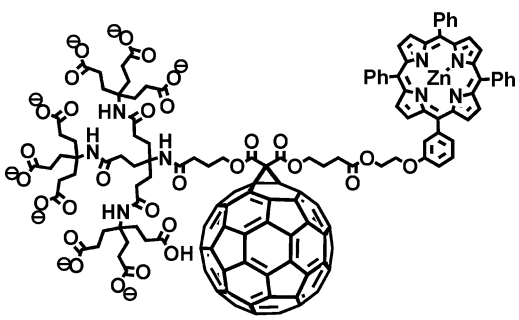

4

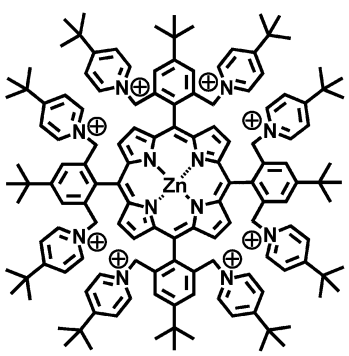

5

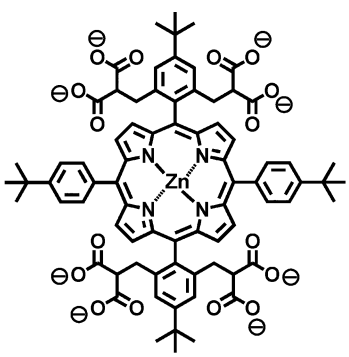

6

been reported to date. However, defined cationic oligoelectrolytes beyond the colored reporter representative **5** are required as additional building blocks for a systematic development and extension of a versatile LbL-concept for the deposition of OEMs. For this purpose we synthesized as a first representative of cationic Newkome-like dendrimer the nonapyridinium salt **2** by esterification of **1** with *N*-(hydroxyethyl)pyridinium bromide (Scheme 1), which is easily available by the reaction of 4-*tert*-butylpyridine with bromoethanol.[18] Dendrimer **2** provides high charge density and keeps its cationic nature independent of the pH. This is in contrast to most of the cationic dendrimers reported so far, which are generated by reversible and pH-dependent protonation of peripheral amino groups and not through irreversible reaction to quaternary ammonium salts.

2. Layer-by-layer assembly of molecular oligoelectrolytes

2.1 Assembly of monolayers. The layers of the oligoelectrolytes **1–6** were deposited on planar fused silica substrates using the alternate dipping method.[1] After charging a glass surface through etching,[19] the substrate was immersed in solutions of the corresponding cationic or anionic electrolytes for 30 minutes. Etching with saturated solutions of KOH leads to deprotonation of the hydroxyl groups on the glass surface and hence to the formation of a negatively charged substrate, which is now ready for the deposition of the electrolytes. For this purpose, we followed two ways, namely, with and without pre-deposition of a polymer electrolyte. As polymer for the pre-deposition of the initial ground layer we choose poly(allylamine hydrochloride) (PAH) as a polycationic component.[19] Subsequently, the negatively charged oligoelectrolytes **1**, **3**, **4**, **6** were deposited. In the case of the chromophore containing electrolytes **3**, **4**, **6** the deposition can easily be followed by UV–Vis spectroscopy (Fig. 1). Oligoelectrolyte **3** involving the pyrene moiety[10] shows three characteristic pyrene bands between 200 nm and 400 nm on the glass substrate (Fig. 1a). In the range of 400–450 nm, the significant Soret-band of the porphyrins within **4** and **6** can be detected (Fig. 1b, 1c), as well as the Q-bands in the range of 550–700 nm.[11,17] In addition, the characteristic absorptions of the fullerene chromophore in **4** can be seen at 254 and 324 (Fig. 1b).[11]

Then we followed also the second way avoiding the pre-deposition of the polymer ground layer. Since the surface of the glass substrate is negatively charged due to the preceding etching step it was possible to directly deposit the positively charged porphyrin **5**. Fig. 2 shows the electronic absorption spectrum of the coated glass slide with the characteristic features of **5** (Soret-band at 442 nm and Q-band at 573 nm).[17,20] Compared to the corresponding spectra recorded in solution, a red shift of 5 nm was observed. Due to the molecular structure of **5** a formation of *J*-aggregates[21,22] is unlikely. Therefore, we attribute the 5 nm shift to a distortion of **5** on the surface.

2.2 Assembly of multilayer systems. Before we investigated the formation of OEMs themselves, we prepared multilayer structures where PAH always served as the cationic component forming subsequent interlayers for comparison. The alternating deposition of the anionic oligoelectrolytes from our substance library with PAH afforded the desired hierarchically ordered structures on glass substrates. This was again demonstrated by absorption spectroscopy. As can be seen, for example, with the alternating deposition of PAH and **4** (Fig. 3) a linear correlation between the number of layers and the absorbance at specific wavelengths is established. After every dipping circle a UV–Vis spectrum of the coated glass substrate was measured. The four spectra shown in Fig. 3a show the increasing intensity of the absorbance with an increasing number of deposited layers. The plot of the maximum absorbance at 439 nm *versus* the number of layers is presented in Fig. 3b and reveals linear correlation. The linear relationship between film thickness and number of layers was already shown for covalent multilayer systems by Vestberg *et al.*[23]

Fig. 4 shows the corresponding data for the deposited layers of porphyrin **6** as a chromophoric reporter electrolyte alternating with those of PAH. In Fig. 4a, UV–Vis spectra after every bilayer are combined. The absorbance grows with the number of bilayers. The linear correlation between the absorbance and the number of layers is demonstrated at 435 and 320 nm (Fig. 4b).

The next step was to demonstrate that OEMs using exclusively oligoelectrolytes as building blocks can be deposited in the same way. Now, both the ground layer and the interlayers consisting of

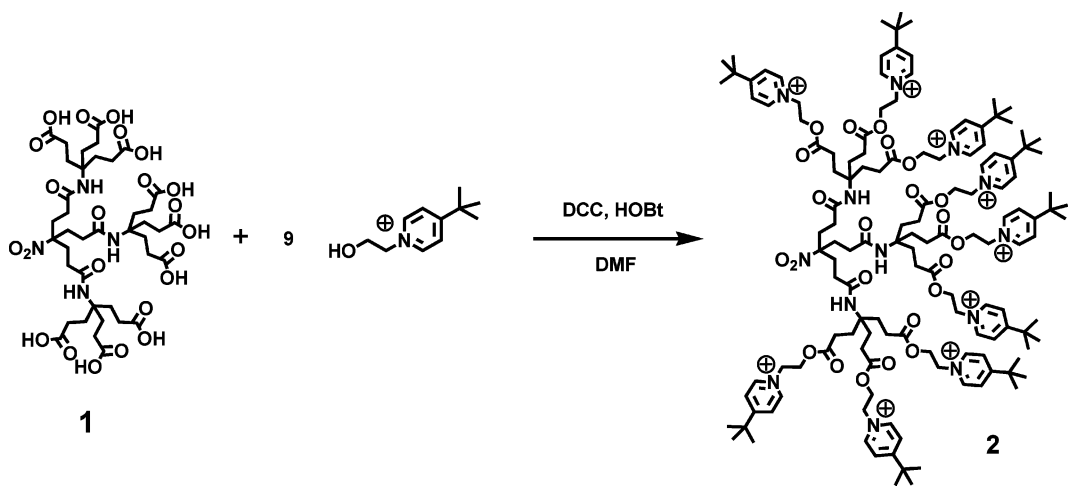

Scheme 1 Synthesis of the novel cationic building block **2** through esterification of **1** (counterions not shown).

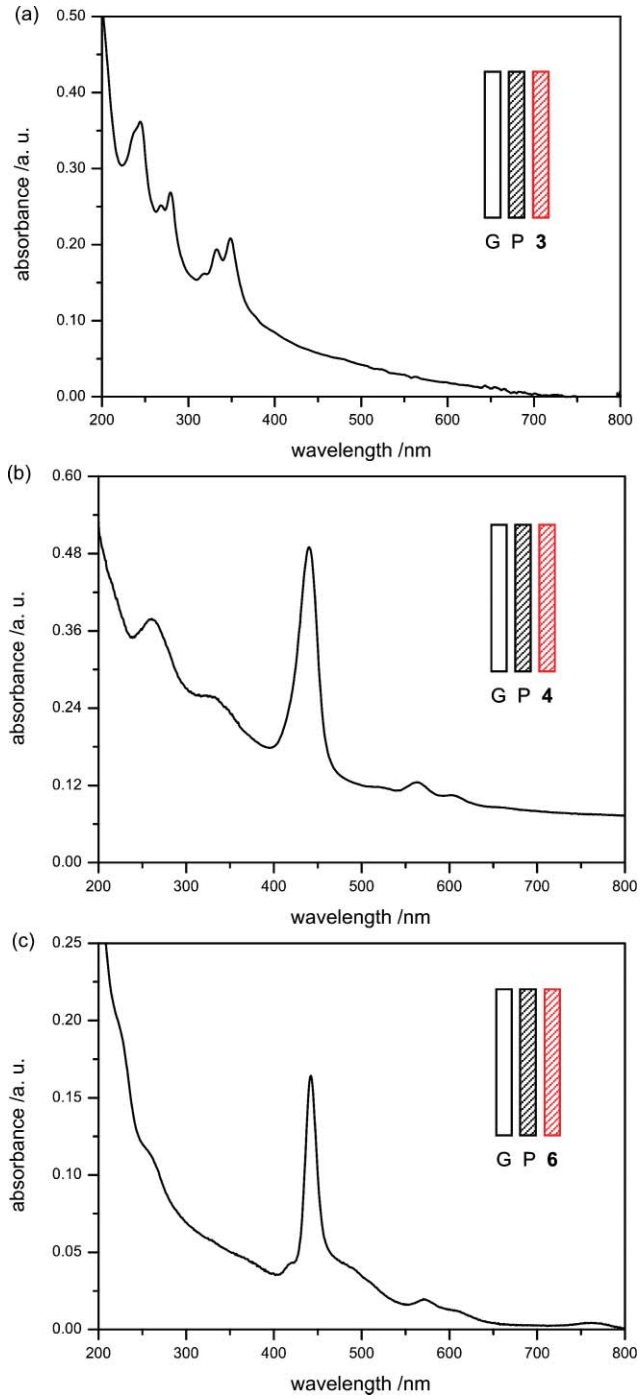

Fig. 1 UV–Vis spectra of molecular oligoelectrolytes **3** (1a), **4** (1b), **6** (1c) coated on an etched glass substrate over a ground layer of PAH (G = glass, P = PAH).

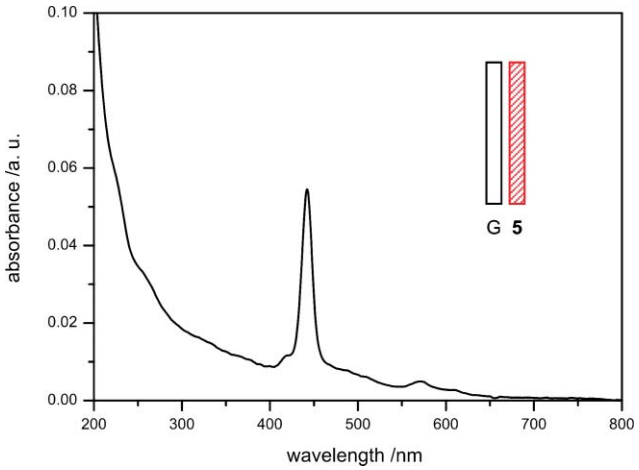

Fig. 2 UV–Vis spectra of one monolayer of porphyrin **5** directly coated on etched glass.

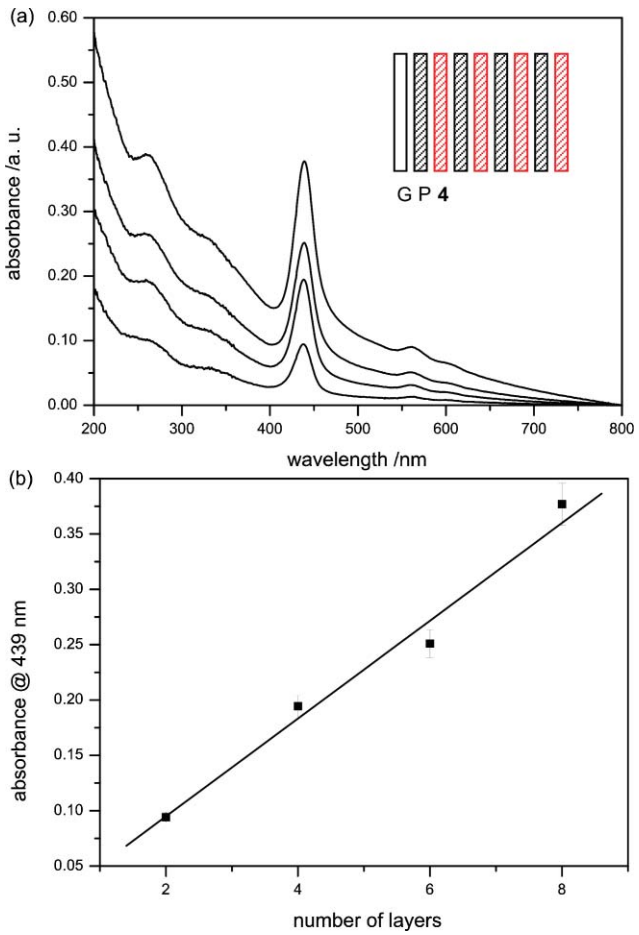

Fig. 3 UV–Vis spectra of a multilayer assembly of 8 layers of PAH (P) and **4** (3a) and correlation of absorbance at 439 nm and number of layers (3b).

PAH were completely left out. In the first example, the ground layer was formed by the deposition of the cationic porphyrin **5** on an etched glass slide. The dendrimer **1** was chosen as an anionic building block. The successful LbL-assembly was monitored by absorption spectroscopy (Fig. 5a). The absorbances at 441 and 571 nm, which are due to the porphyrin chromophore in **5**, rise linearly with an increasing number of layers (Fig. 5b).

In order to investigate initial approaches to possible application of OEMs as potential drug delivery systems, we employed as an anionic building block for the LbL-formation, a biologically active agent **7** belonging to the class of bisphosphonates used to medicate bone metastasis or hypercalcemia of malignancy caused by excess bone resorption.[24]

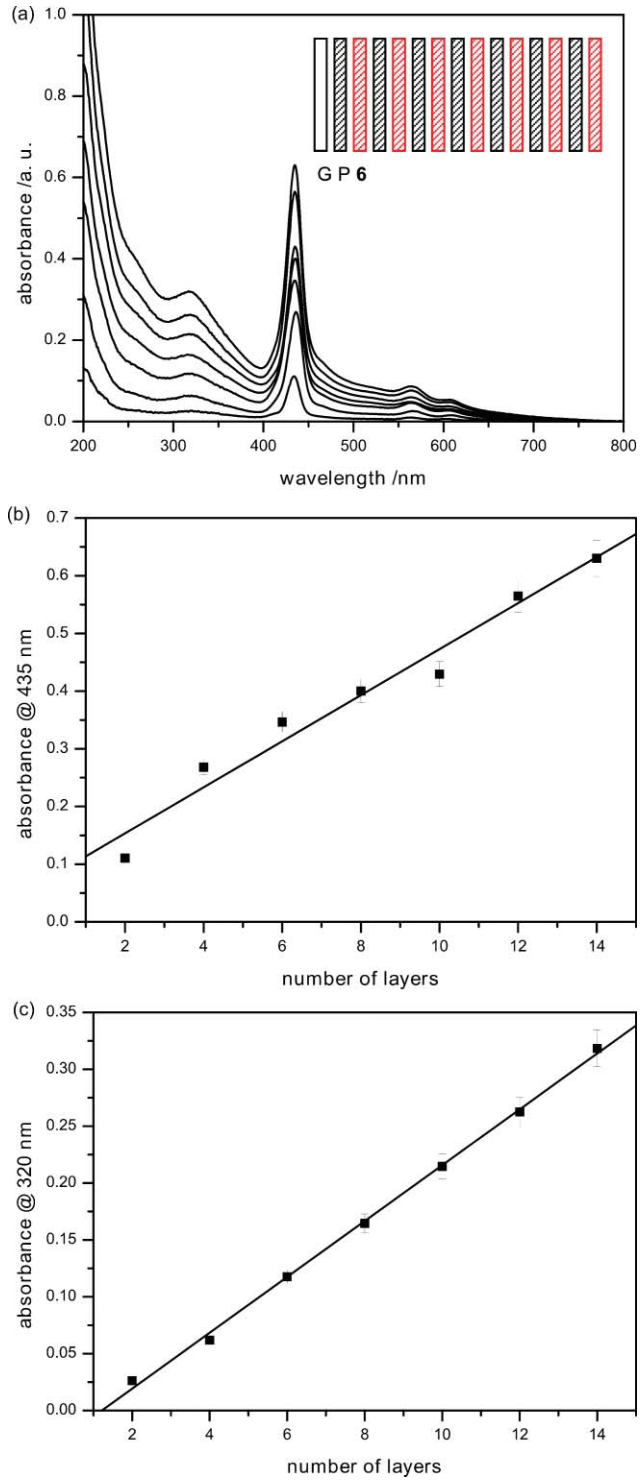

Fig. 4 UV–Vis spectra of a multilayer assembly of 14 layers of PAH (P) and **6** (4a) and correlation of absorbance at 435 nm and 320 nm and number of layers.

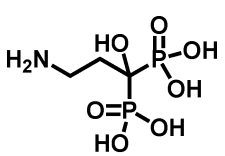

7

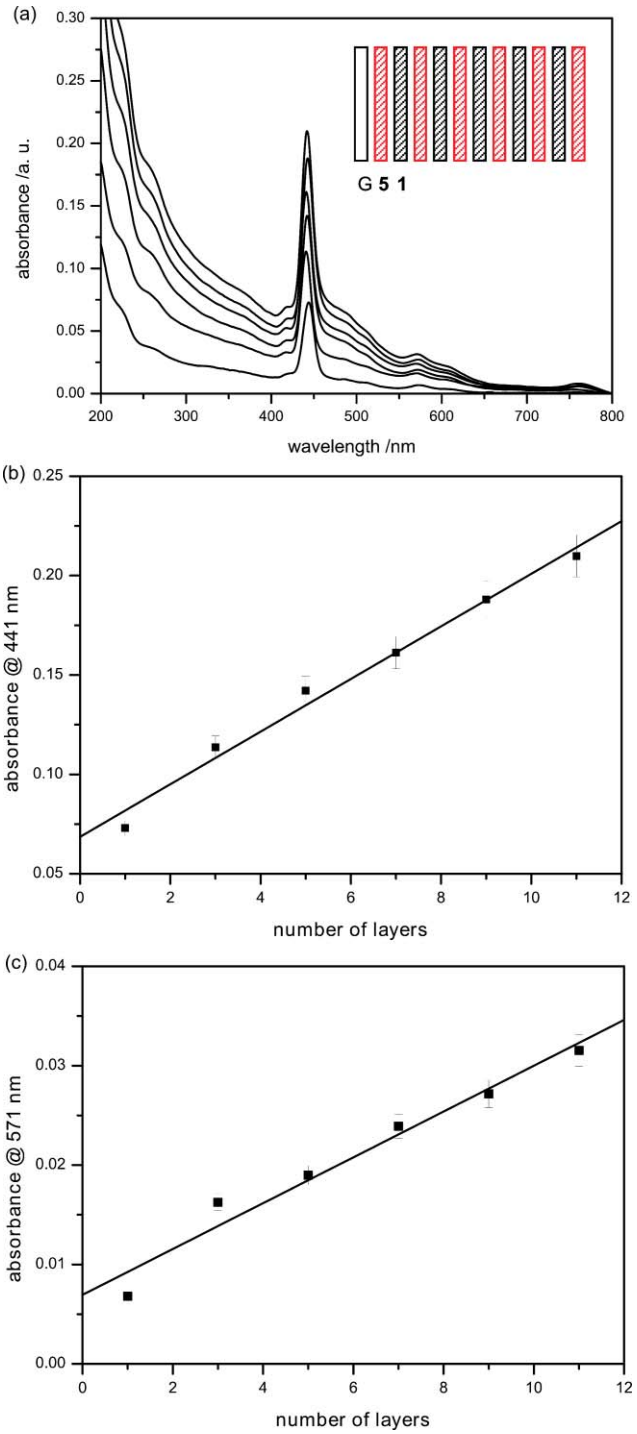

Fig. 5 UV–Vis spectra of a multilayer assembly of 11 layers of **5** and **1** (5a) and linear correlation of absorbance at 441 nm and 571 nm and number of layers.

Again we are in the position to abandon polymeric components from this proto-type drug delivery system. As porphyrin **5** serves as cationic component and at the same time as reporter electrolyte, the detection of the anionic agent occurs indirectly. We observe an increasing absorbance of **5** with increasing number of layers. This allows for the regulation of the amount of deposited pamidronate **7** by the number of layers. The linearity between the number of layers and absorbance at 442 nm is shown in Fig. 6b.

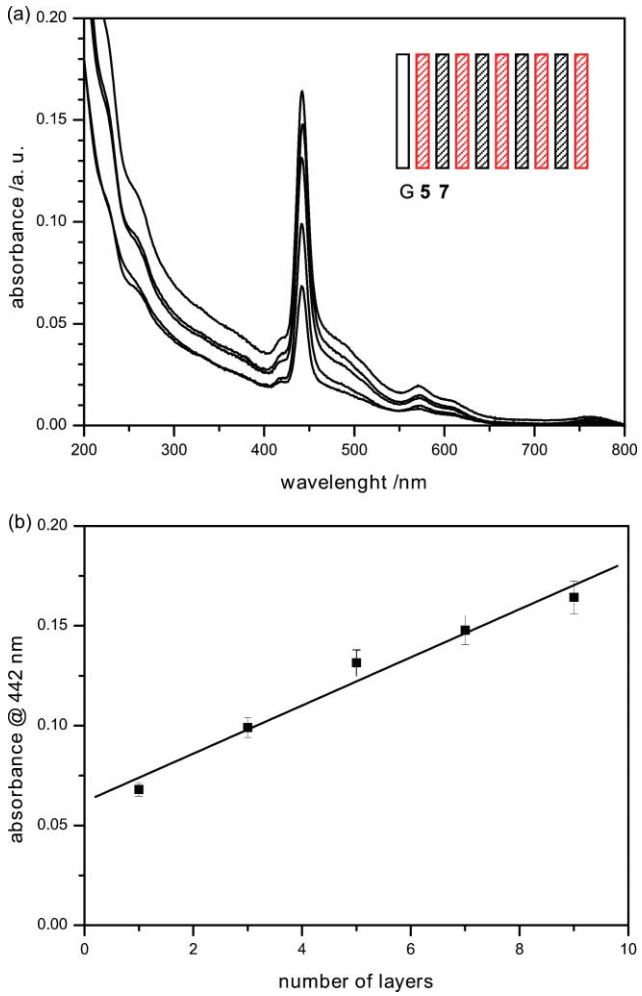

Fig. 6 UV–Vis spectra of the assembly of 9 layers of **5** and pamidronate (**7**) (6a) and correlation of absorbance at 442 nm and number of layers.

The linear correlation of the absorbance of the oligoelectrolytes with the number of deposited layers serves as clear proof that the LbL-method is a suitable concept for the formation of OEMs. With every dipping circle the same amount of substance is deposited on the glass slide. In order to determine the exact amount of oligoelectrolyte that is deposited on the surface, an etched glass slide was dipped into a solution of the cationic porphyrin **5** and then washed with water for two minutes and subsequently dried under atmospheric conditions. Then an absorption spectrum of the sample was taken. The maximum absorption is found at 442 nm (Soret band) with a value A of 0.0715 (Fig. 2). Using Lambert–Beers law and taking the extinction coefficient of **5** ($\varepsilon \approx 430.000\ M^{-1}cm^{-1}$)[20] from solution, the Avogadro constant N_A and a roughness factor k_r of 1.3 for glass, a mean molecular area[21] (mma) of 2.6 nm^2 arises (eqn (1)). This calculation follows the fact that mma is the inversed molecular surface density, which in turn can be calculated by multiplying the concentration with the layer thickness.[21]

$$mma = \frac{k_r \varepsilon}{N_A A} \quad (1)$$

The minimum structure of porphyrin **5** was calculated on the PM3 level[25] and resulted in a dimension of 2.9 nm^2 for the molecule (Fig. 7). This corresponds quite nicely to the measured value and approves the theoretical considerations that it is exclusively monolayers that are built due to electrostatic repulsion.

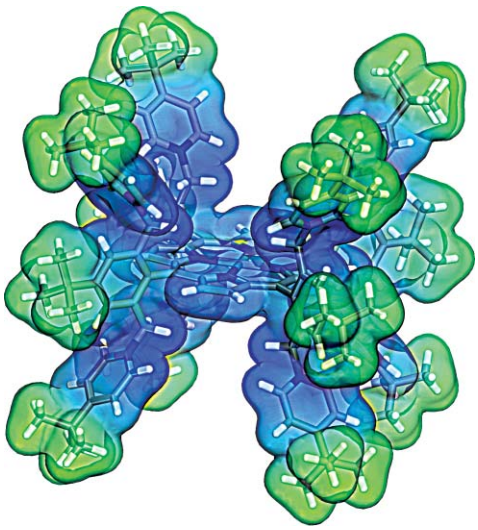

Fig. 7 PM3-minimized structure[25] of compound **5**.

3. Degradation

Controlled degradation experiments were performed in a vial containing 10 mL of phosphate buffer pH 7 (see experimental section). The pre-coated and dried glass slides were immersed and samples of the buffer solution were taken at certain times to measure fluorescence spectra of the released reporter porphyrins. We employed the much more sensitive fluorescence spectroscopy instead of absorption spectroscopy because the concentrations of the released reporter dyes can be estimated to be at most 10^{-8} mol L^{-1}. The correlation of the emission intensities at a specific detection wavelength with degradation time allows for the determination of the kinetics of the degradation process. Complete degradation of the OEMs was achieved when no further increase of the concentration of the reporter electrolyte in solution is monitored and a saturation level is reached. For a single monolayer of **5** on glass, this situation is reached after about 15 minutes only. The corresponding degradation of the monolayer on the glass substrate is shown in Fig. 8 and follows an exponential first order decay with a rate constant of 4.38.

To investigate degradation of OEMs, we used films consisting of eight layers as model cases. Seven layers consisted of colorless dendritic oligoelectrolytes **1** and **2** whereas one layer of the porphyrin **5** was deposited in a selected position between those of **1** and **2**. In this way, **5** served again as the reporter electrolyte to monitor the degradation process. The position of the reporter layer was varied from the very inside to the last but one layer. The monitored time dependent release of **5** out of the [7,8] system (position of the reporter layer is 7th out of 8) shows that the concentration of the porphyrin rises very quickly and reaches saturation after 30 minutes only (Fig. 9a).

The [3,8] system (reporter layer is the 3rd out of 8) shows analogous behavior, but over a considerably longer period of time. The slower ascent of reporter concentration in solution and the decelerated saturation shows that the release of the

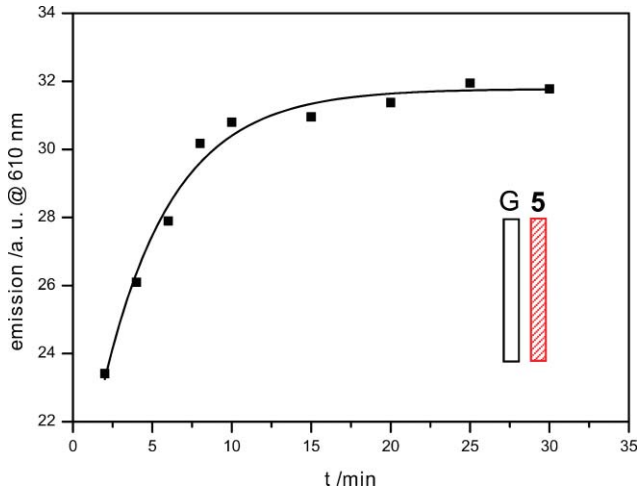

Fig. 8 Degradation kinetics of a monolayer of **5** on glass (G), fitting a graph of first order.

reporter proceeds more slowly (Fig. 9b). We believe that this behavior arises from the inner position of the reporter electrolyte layer and suggests that it is protected by the outer layers of **1** and **2**. To corroborate this assumption, we also investigated the corresponding [1,8] system where the innermost layer is represented by the reporter electrolyte **5**. In this case, the release was indeed very slow and the saturation of the concentration occurs at a very late point of time (Fig. 9c). After three hours, the reporter concentration in solution still increases. These data nicely support our assumption. The different rates of degradation can be monitored by the constant factors m_1 and m_2 (eqn (2)) of the fitting graphs of the experimental degradation plots. The smaller the values, shown in Table 1, the faster the reaction proceeds. All multilayer degradation kinetics showed a second order exponential decay.

$$y = A_1 e^{\left(\frac{-x}{m_1}\right)} + A_2 e^{\left(\frac{-x}{m_2}\right)} + y_0 \quad (2)$$

In all OEM degradation experiments, we detected reporter electrolytes in solution from the very beginning. This implies that the degradation process is not only due to a subsequent peeling of one layer after another in a regular degradation directed from the top to the bottom. It is very likely that there are imperfections such as holes in the OEMs, which serve as channels for the immediate desorption of reporter electrolytes **5** located also in inner layer positions. For PEMs these two modes of erosion are known as top-down pathway and bulk-type pathway.[6] We showed that the bulk-type reaction only occurs when a multilayer system is considered. Only in this case pitting is possible. The degradation of simply one layer, where pitting is impossible, accordingly follows an exponential first order decay.

Table 1 Degradation rate constants of the different multilayer systems

Multilayer system	m_1	m_2
[7,8]	0.61	31.55
[3,8]	5.02	60.11
[1,8]	18.48	149.38

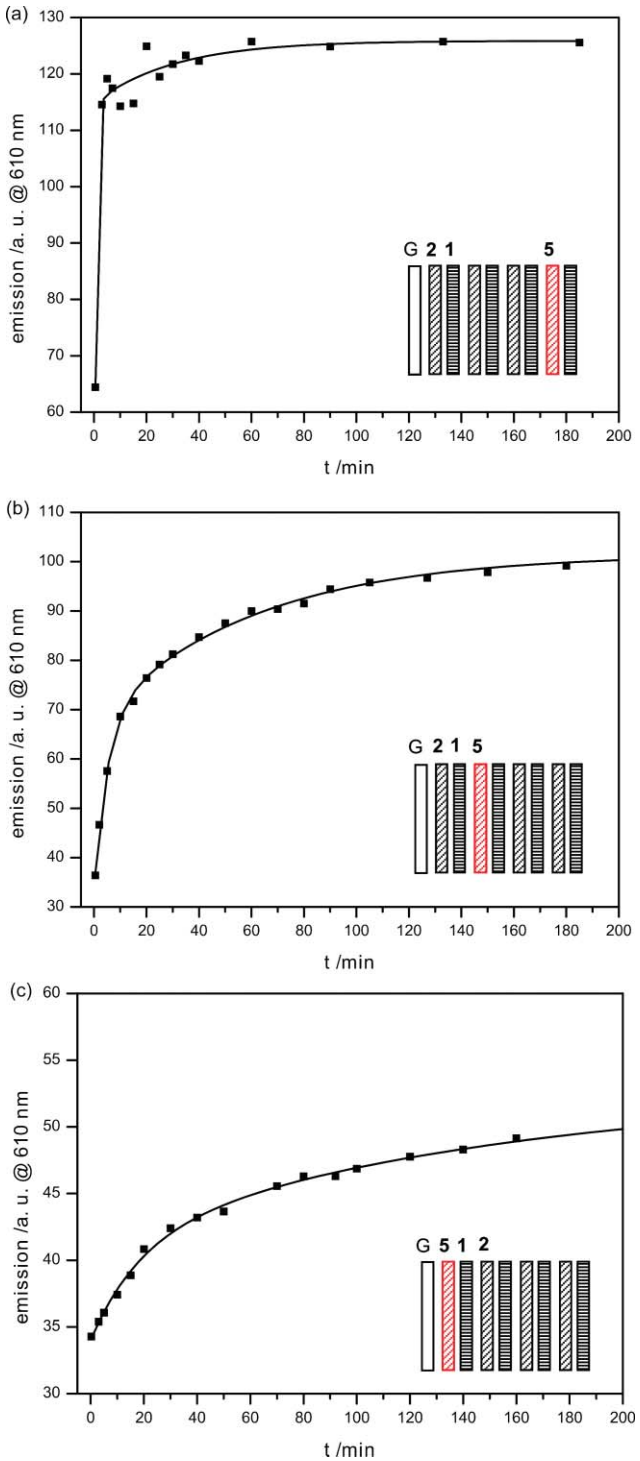

Fig. 9 Degradation kinetics of multilayer systems [7,8] (9a), [3,8] (9b) and [1,8] (9c), fitting graphs of second order.

Conclusion

In this study we examined the assembly and degradation behavior of OEMs self assembled by layer-by-layer deposition of oligoelectrolytes. Next to colorless oligoelectrolytes we have employed representatives involving chromophores, in particular porphyrins. This allows for the systematic observation of both assembly and disassembly of the OEMs using optical spectroscopy,

where chromophore containing building blocks serve as reporter electrolytes. The oligoelectrolytes used in this study are perfectly monodisperse. Moreover, their structure and properties can be varied in a broad range by applying new synthesis protocols including those developed in dendrimer chemistry. This offers a number of advantages compared with the classical layer-by-layer concept using polymer electrolytes. The OEMs investigated in this study were built in a consistent, monomolecular matter and show linear correlation between the absorption and the number of layers. Using the concept of reporter electrolytes, we have introduced for the first time also the use of non-chromophoric oligoelectrolytes as building blocks for OEMs. Moreover, we have investigated for the first time the degradation behavior of OEMs. We demonstrated that two different mechanisms of degradation proceed at the same time. The direct degradation is accompanied by a second release mechanism. These studies show that specifically loaded and arranged OEMs can be used to develop time profiles for the time dependent release of active components, which could be of importance, for example, for drug delivery applications.

Experimental

General considerations

Silicon substrates (4.5 cm × 1 cm) were etched in a saturated solution of KOH in isopropanol and water (all HPLC-grade from Fluka) for 30 minutes.[19] After that, the samples were rinsed with water until pH neutrality. Thin film deposition was observed *via* UV–Vis spectroscopy using an Analytik Jena Specord S600 spectrometer. Degradation measurements were performed in buffer pH 7 and recorded by fluorescence spectroscopy with a Shimadzu Spectrofluorometer RF-5301 PC.

Preparation of polyelectrolyte solutions

Oligoelectrolytes **1**,[15,16] **3**,[10] **4**,[11] **5** and **6**[14,17] were synthesized following the published descriptions. Millipore water (conductance smaller than 2 μS cm^{-1}) was obtained from Fluka and was used for the washing steps, the preparation of the buffer and for the preparation of the oligoelectrolyte solutions. The concentration was adjusted to 10^{-2} M in buffer pH 7. The buffer was prepared from 0.1 M KH_2PO_4 and 0.1 M NaOH solution. This buffer was also used for the degradation experiments. All solutions were filtrated trough a Millipore Millex-GP hydrophilic filter with a pore size of 0.22 μm.

Polyelectrolyte deposition

All oligoelectrolyte thin films were constructed according to the alternate dipping method.[1] Substrates were submerged in a solution of a cationic oligoelectrolyte for 30 minutes followed by a washing step with water. This procedure was repeated with a solution of an anionic oligoelectrolyte. The cascade was repeated until the required number of layers was achieved.

Measurement of thin film construction

The assembly of the layers was monitored by the incorporation of chromophoric reporter electrolytes as film components. Every second layer was built by such a molecule. After every second layer, a UV–Vis spectrum was recorded and the absorption at a specific wavelength was correlated with the number of layers.

Measurement of thin film degradation

The film degradation was studied with multilayer systems of achromatic molecules. A single cationic dendrimer layer was substituted by a fluorescent, cationic porphyrin layer. All film degradation studies were performed as follows. Films were immersed in 10 mL of a buffer solution (pH 7). At designated times an assay was taken from the solution and investigated by fluorescence spectroscopy. The samples were put back in solution to ensure a constant volume. The fluorescence emission at different wavelengths was correlated with the time when the sample was taken.

9 Cascade:nitromethane[3]:(2-aza-3-oxopentylidyne):2-(4-*tert*-butyl)pyridiniumethyl-propanoate bromide (2)

A solution of 9-cascade:nitromethane[3]:(2-aza-3-oxopentylidyne):propanoic acid **1** (0.21 g, 0.22 mmol) and HOBt (0.54 g, 3.96 mmol) in dry DMF (20 cm^3) is cooled to 0 °C and DCC (0.82 g, 3.96 mmol) is added. After 30 min, 2-hydroxyethyl-(4-*tert*-butyl)-pyridinium-bromide[18] (1.03 g, 3.96 mmol) is added and the solution is stirred for 7 days at room temperature. Precipitated DCU is filtered off and the solvent is evaporated under reduced pressure. The residue is dissolved in MeOH and precipitated with acetone. The precipitation is repeated three times to give **2** (0.18 g, 26%) as slightly yellowish solid. (Found: C, 52.5; H, 6.6; N, 6.2. $C_{139}H_{204}Br_9N_{13}O_{23}$ + 1H_2O + 1DMF requires C, 52.7; H, 6.6; N, 6.1%); ν_{max}(film)/cm^{-1} 3412, 3254, 2968, 1733, 1640, 1536, 1459, 1158, 1116, 1042 and 849; δ_H (400 MHz; MeOD-d_4) 1.44 (s, 81 H, CH_3), 1.92 (br s, 18 H, C$H_2$$CH_2$COO), 2.28 (br s, 12 H, CH_2CH_2CON), 2.34 (br s, 18 H, CH_2CH_2COO), 4.58 (br t, 18 H, CH_2O), 4.96 (br t, 18 H, CH_2N), 8.22 (d, J = 6.84 Hz, 18 H, Ar-H), 9.03 (br d, 18 H, Ar-H); δ_C (100 MHz; MeOD-d_4) 29.3, 30.2, 30.4 (24 C, dendritic-C), 30.5 (27 C, CH_3), 37.8 (9 C, $C(CH_3)_3$), 58.8 (3 C, CNH), 60.8 (9 C, CH_2O), 64.1 (9 C, CH_2N), 88.6 (1 C, CNO_2), 126.9 (18 C, Ar-C), 146.2 (18 C, Ar-C), 173.5 (9 C, COO), 173.9 (3 C, CONH), 174.4 (9 C, Ar-C); m/z (FAB) 3065 (M^+ − Br); m/z (ESI) 1492 (M^{++} − 2Br).

References

1 G. Decher, *Science*, 1997, **277**, 1232.
2 N. G. Hoogeveen, M. A. C. Stuart, G. J. Fleer and M. R. Boehmer, *Langmuir*, 1996, **12**, 3675.
3 Z. Tang, Y. Wang, P. Podsiadlo and N. A. Kotov, *Adv. Mater.*, 2006, **18**, 3203.
4 A. J. Chung and M. F. Rubner, *Langmuir*, 2002, **18**, 1176.
5 A. J. Khopade and F. Caruso, *Nano Lett.*, 2002, **2**, 415.
6 D. M. Lynn, *Adv. Mater.*, 2007, **19**, 4118.
7 S. Y. Park, M. F. Rubner and A. M. Mayes, *Langmuir*, 2002, **18**, 9600.
8 M. Brettreich, S. Burghardt, C. Böttcher, T. Bayerl, S. Bayerl and A. Hirsch, *Angew. Chem., Int. Ed.*, 2000, **39**, 1845.
9 M. Braun, S. Atalick, M. Guldi Dirk, H. Lanig, M. Brettreich, S. Burghardt, M. Hatzimarinaki, E. Ravanelli, M. Prato, R. Van Eldik and A. Hirsch, *Chem.–Eur. J.*, 2003, **9**, 3867.
10 A. Ebel, W. Donaubauer, F. Hampel and A. Hirsch, *Eur. J. Org. Chem.*, 2007, 3488.
11 C. Kovacs and A. Hirsch, *Eur. J. Org. Chem.*, 2006, 3348.
12 U. Hartnagel, D. Balbinot, N. Jux and A. Hirsch, *Org. Biomol. Chem.*, 2006, **4**, 1785.

13 I. Zilbermann, A. Lin, M. Hatzimarinaki, A. Hirsch and D. M. Guldi, *Chem. Commun.*, 2004, 96.
14 D. M. Guldi, I. Zilbermann, G. Anderson, A. Li, D. Balbinot, N. Jux, M. Hatzimarinaki, A. Hirsch and M. Prato, *Chem. Commun.*, 2004, 726.
15 G. R. Newkome, R. K. Behera, C. N. Moorefield and G. R. Baker, *J. Org. Chem.*, 1991, **56**, 7162.
16 G. R. Newkome, A. Nayak, R. K. Behera, C. N. Moorefield and G. R. Baker, *J. Org. Chem.*, 1992, **57**, 358.
17 N. Jux, *Org. Lett.*, 2000, **2**, 2129.
18 D. Kuhnen-Clausen, I. Hagedorn and R. Bill, *J. Med. Chem.*, 1979, **22**, 177.
19 S. Fujita and S. Shiratori, *Nanotechnology*, 2005, **16**, 1821.
20 D. Balbinot, *Dissertation*, 2006, Universität Erlangen.
21 V. Chukharev, T. Vuorinen, A. Efimov, N. V. Tkachenko, M. Kimura, S. Fukuzumi, H. Imahori and H. Lemmetyinen, *Langmuir*, 2005, **21**, 6385.
22 T. Vuorinen, K. Kaunisto, V. Tkachenko Nikolai, A. Efimov, H. Lemmetyinen, S. Alekseev Alexander, K. Hosomizu and H. Imahori, *Langmuir*, 2005, **21**, 5383.
23 R. Vestberg, M. Malkoch, M. Kade, P. Wu, V. V. Fokin, K. B. Sharpless, E. Drockenmuller and C. J. Hawker, *J. Polym. Sci., Part A: Polym. Chem.*, 2007, **45**, 2835.
24 H. Kajiwara, T. Yamaza, M. Yoshinari, T. Goto, S. Iyama, I. Atsuta, A. Kido Mizuho and T. Tanaka, *Biomaterials*, 2005, **26**, 581.
25 *Materials Studio*®, Version 2.2.1, © 2002, Accelrys Inc., www.materials-studio.com.